ASTROBIOLOGY
Volume 22, Number 4, 2022

DOI: 10.1089/ast.2021.0138

Infrared Spectral Intensities of Amine Ices, Precursors to Amino Acids

Reggie L. Hudson,[1,i] Yukiko Y. Yarnall,[1,2] and Perry A. Gerakines[1,ii]

Abstract

Here, we address the paucity of infrared (IR) spectral data needed to quantify low-temperature experiments with amine ices, such as the formation of amino acids, by reporting new IR results on solid phases of methylamine (CH_3NH_2) and ethylamine ($CH_3CH_2NH_2$), precursors to glycine and alanine, respectively. Mid-IR band strengths and absorption coefficients for CH_3NH_2 and $CH_3CH_2NH_2$, in both amorphous and crystalline forms, are presented, along with measurements of a density and refractive index (670 nm) for each. For these same compounds, we also have calculated IR optical constants, and they are being made available in electronic form. Some applications of our new results are described along with proposals for future investigations. Suggestions are made related to the methods employed in such work, and particularly to the application of Beer's Law to the IR study of compounds of astrobiological interest. Comments are also included on the methods used, and the results presented in a recently published work on amino-acid IR intensities. Key Words: Pre-biotic chemistry—Extraterrestrial organic compounds—Laboratory investigations—Infrared spectroscopy—Ice. Astrobiology 22, 452–461.

1. Introduction

Planetary bodies and their chemical and biological constituents derive from interstellar materials, and so the study of organics in the interstellar medium is of astrobiological interest. Our own investigations of interstellar chemistry have been documented in a long series of papers on low-temperature chemistry, focusing on how ionizing radiation can initiate chemical changes in icy solids at temperatures from about 10 to 200 K (Materese *et al.*, 2021). To aid in the quantification of such work, covering both laboratory research and astronomical observations, we have measured the infrared (IR) spectra of a variety of organic and inorganic compounds of astrobiological relevance.

Along these lines, the paper of Iglesias-Groth and Cataldo (2021) recently published here is of particular interest as it aims at quantifying IR spectra. Those authors presented reference IR spectra and intensities for five amino acids, with each compound being isolated in an IR-transparent matrix and its mid-IR spectrum shown at three temperatures. The IR intensities were reported for absorbance peaks and as integrations to give band strengths. Such work is similar to our own (Moore *et al.*, 2010; Hudson *et al.*, 2014a, 2014b, 2017), and for that reason we wish to offer some comments, cautions, and suggestions. To illustrate our comments, we present new results from our recent IR study of solid methylamine (CH_3NH_2) and ethylamine ($CH_3CH_2NH_2$).

The astrobiological and astrochemical interest in and importance of CH_3NH_2 and $CH_3CH_2NH_2$ are readily found in the literature. Methylamine is an interstellar molecule (Kaifu *et al.*, 1974), and it has been found in Stardust samples and the coma of comet 67P/Churyumov-Gerasimenko (Glavin *et al.*, 2008; Altwegg *et al.*, 2016). Radiation-induced reactions of CO_2 + methylamine mixtures are one path to the amino-acid glycine (de la Paz and Getoff, 1966). Simialr to methylamine, ethylamine also has been found in the coma of comet 67P/Churyumov-Gerasimenko and in Stardust samples (Glavin *et al.*, 2008; Altwegg *et al.*, 2016).

[1]Astrochemistry Laboratory, NASA Goddard Space Flight Center, Greenbelt, Maryland, USA.
[2]Universities Space Research Association, Greenbelt, Maryland, USA.
[i]ORCID ID (https://orcid.org/0000-0003-0519-9429).
[ii]ORCID ID (https://orcid.org/0000-0002-9667-5904).

This compound's reaction with CO_2, by radiolysis or photolysis, produces the amino acid alanine (Getoff and Schenck, 1967). Both these amines also are well documented in a variety of meteorites (Aponte *et al.*, 2017).

Our interest in CH_3NH_2 and $CH_3CH_2NH_2$ derives from our studies of chemical reactions in icy solids that can make or destroy amino acids (Hudson *et al.*, 2009; Gerakines and Hudson, 2013). For example, we showed that a residue formed by the proton irradiation of a CO_2 + *sec*-butylamine ice at 10 K, followed by warming to room temperature, contained isovaline, a meteoritic amino acid. However, we have found that much of the relevant solid-phase laboratory work in the literature, including our own, is hindered by a lack of background measurements with which to produce quantitative results.

As another example, Holtom *et al.* (2005) studied the solid-phase CO_2 + CH_3NH_2 reaction to make glycine, but the source and accuracy of those authors' IR band strengths for CH_3NH_2 is unknown, making determinations of reactant mass and reaction yield uncertain. Those same authors' IR band strengths later were used by Vinogradoff *et al.* (2013), who also studied CH_3NH_2 reactions, and by Mahjoub and Hodyss (2018), who made a peptide precursor from CH_3NH_2 + OCS ices. Turning to $CH_3CH_2NH_2$, the situation is worse as no reliable IR solid-phase band strengths appear to be available. Danger *et al.* (2011) investigated solid-phase nitrile formation from *ethyl*amine, but they adopted band strengths of *methyl*amine as nothing else was available. Therefore, one goal of the present article is to correct this situation by reporting new IR results that can be used to quantify all such work with amines, precursors to amino acids.

2. Beer's Law and IR Intensities in Ices

Determinations of IR spectral intensities in icy solids have been described in our recent papers, with some of the procedures used going back to the 1950s (Swenson *et al.*, 1959). Briefly, a series of samples is prepared with a range of either concentrations or path lengths, the absorbance spectrum of each sample is recorded, and the IR bands of interest are integrated or absorbance peak heights are measured. In our own work, we vary path length and measure IR absorbances. Equations (1) and (2) are then used to plot peak height or integrated absorbance as a function of path length (h), for samples of the same number density (ρ_N).

$$Absorbance = \left(\frac{\alpha'}{2.303}\right) h. \quad (1)$$

$$\int_{band} (Absorbance)\, d\tilde{\nu} = \left(\frac{\rho_N A'}{2.303}\right) h. \quad (2)$$

The desired result is data points that form a line going through the graph's origin. The line's slope equals (α'/2.303) from Equation (1) and (ρ_N A'/2.303) from Equation (2), where α' is a peak's IR absorption coefficient and A' is the integrated feature's IR band strength. The factor of ln(10) $\approx$ 2.303 converts the common logarithmic scale of most commercial IR spectrometers to a natural log scale. These equations are, of course, just versions of Beer's Law: Absorbance is proportional to the number of absorbers along an optical path. Neither Equation (1) nor (2) can be taken *a priori* to apply to an icy solid, but they must be demonstrated by measurements that give a linear relation and an intercept near zero from which either α' or A' can be extracted.

We emphasize that Equations (1) and (2) cannot be taken for granted, but they must be demonstrated by preparing and recording spectra of multiple samples, plotting the data, and examining them for linearity and a near-zero intercept before extracting α' and A'. Unfortunately, the mid-IR intensities in the five data tables of Iglesias-Groth and Cataldo (2021) all appear to have been obtained from a single IR sample of each amino acid. No series of solid samples were described with measurements made and results plotted to test or show adherence to Beer's Law. This is equivalent to measuring an IR feature in one spectrum, assuming that Beer's Law holds, and then drawing a line between the resulting data point and the origin of a coordinate system, amounting to a one-point calibration curve. However, the origin of a graph is not a data point, and it is difficult to see how calibrations based on a single point can be reliable. A better approach to the problem is to prepare samples with either a range of thicknesses or amino-acid concentrations, and then to measure the spectrum of each.

We also note that no temperatures were given for the solids for which Iglesias-Groth and Cataldo (2021) tabulate peak positions, an important omission. However, each of the authors' tables includes at least four equations relating IR peak position to temperature, which permit temperature calculations from the peaks listed for each amino acid. Using the four equations presented for glycine gives a sample temperature of 300, 388, 310, and 346 K, a wide variation. Even more striking is that the phenylalanine sample's temperature is calculated as about −1100 K when using the 6.39 μm feature's equation, but about 15,000 K when calculated with the 6.86 μm band.

Our experience is that quantitative IR spectroscopic measurements are difficult and time-consuming, but the results are important not only for determining molecular abundances of organics in extraterrestrial and laboratory ices, but also for lab-to-lab comparisons to build confidence in published results and to uncover possible errors. Therefore, in this article we describe our recent quantitative work on IR intensities of two astrobiologically relevant compounds, offering suggestions for applications and future studies.

Note that we have intentionally avoided initiating a new investigation of amino acids, although we have experience with these compounds through several projects (Gerakines *et al.*, 2012; Gerakines and Hudson, 2013, 2015). We leave it to others to apply our suggestions to amino acids.

3. Experimental Methods

All reagents used in this work were purchased from Sigma Aldrich (now MilliporeSigma). Each was research grade and used as received aside from routine degassing, vacuum-line distillation, and drying.

The laboratory methods and procedures followed were identical to those described in several of our recent papers (Hudson *et al.*, 2021). Briefly, ice samples were made by vapor-phase deposition onto a pre-cooled substrate inside a vacuum chamber ($\sim 10^{-8}$ torr). Deposition temperatures

Table 1. Refractive Indices, Densities, and Molar Refractions of Ices

	Amorphous ices			*Crystalline ices*		
Ice	n_{670}	ρ (g/cm^3)	R_M (cm^3/mol)	n_{670}	ρ (g/cm^3)	R_M (cm^3/mol)
Ammonia NH_3	1.33	0.680	5.11	1.44	0.833	5.39
Ethane CH_3CH_3	1.41	0.663	11.12	1.50	0.778	11.37
Methylamine CH_3NH_2	1.38	0.732	9.81	1.46	0.861	9.88
Methanol CH_3OH	1.30	0.779	7.60	1.44	1.023	7.61
Propane $CH_3CH_2CH_3$	1.36	0.653	14.79	1.48	0.797	15.72
Ethylamine $CH_3CH_2NH_2$	1.35	0.662	14.62	1.51	0.924	14.54
Ethanol CH_3CH_2OH	1.32	0.739	12.37	1.47	0.989	14.91

See the text for uncertainties. Sources of n_{670} and ρ are NH_3: this work at 18 and 100 K; CH_3CH_3: this work at 15 and 60 K; CH_3NH_2: this work at 18 and 110 K; CH_3OH: Hudson *et al.* (2020) at 15 K and this work at 120 K; $CH_3CH_2CH_3$: Hudson *et al.* (2021) at 15 and 65 K; $CH_3CH_2NH_2$: this work at 18 and 100 K; CH_3CH_2OH: Hudson *et al.* (2020) at 15 K and this work at 120 K. An extra significant figure has been carried for several values of R_M.

typically were 10 K for amorphous ices and 100 K for crystalline ones. Interference fringes recorded during ice growth gave each sample's thickness (*vide infra*), with values ranging from about 0.25 to 3 μm. Mid-IR transmission spectra of the resulting ices were recorded with a resolution of 1 cm^{-1} from about 5000 to 400 cm^{-1}, typically with 200 scans per spectrum using a Thermo iS50 spectrometer with a DTGS detector. Baselines were straightened manually if needed, and IR bands were integrated and peak heights were measured.

For determinations of ice thickness (h), Equation (3) was used.

$$h = \frac{N_{fr}\lambda}{2\sqrt{n^2 - \sin^2\theta}}, \tag{3}$$

Here, N_{fr} was the number of interference fringes recorded during ice formation, n was the ice's refractive index at 670 nm, and $\theta \approx 0°$ was the angle between the incident laser beam and a line drawn perpendicular to the substrate (Heavens, 1955/2011).

The IR band strengths (A') and absorption coefficients (α') for peaks were found with the Beer's Law plots already described by Equations (1) and (2). Graphs of absorbance peak heights as a function of ice thickness were linear with slopes equal to (α'/2.303), from which α' values were found according to Equation (1). Similarly, graphing band areas as a function of ice thickness gave linear plots from which, using Equation (2), A' values were calculated. Two examples are given in the Results section.

Inspection of Equations (1) and (2) shows that their use requires ice thickness (h) to be measured, which according to Equation (3) requires a reference index of refraction (n). The latter was found in separate measurements with two-laser interferometry in a UHV chamber ($\sim 10^{-10}$ torr), as described in the work of Hudson *et al.* (2017). Simultaneously, we used an INFICON quartz-crystal microbalance to obtain each ice's density (ρ), again as in the work of Hudson *et al.* (2017). The lasers employed for thickness and n measurements had $\lambda = 670$ nm, and so from here on we use n_{670} to designate the visible-region refractive indices we measured.

We use α' and A' to distinguish absorption coefficients and integrated band strengths, respectively, which were found either directly by using IR spectra or optical constants $n(\tilde{\nu})$ and $k(\tilde{\nu})$ from the corresponding quantities α and A calculated only from optical constant(s) $k(\tilde{\nu})$. See the works of Hudson *et al.* (2014a), Hudson *et al.* (2014b), and references therein. The conversion for absorbance intensities of peaks between the present work and that of Iglesias-Groth and Cataldo (2021) is $\alpha' = (\ln 10)(\varepsilon\, c)$, where ε is molar absorptivity and c was used by those authors to denote each sample's amino-acid concentration in terms of molarity. Also note that in this article we use the expression "Beer's Law" for convenience, but several names are associated with this relation's historical development (Mayerhoöfer *et al.*, 2020).

4. Results

Table 1 lists the methyl- and ethylamine refractive indices and densities measured for this work, each in triplicate or better so as to reduce standard errors in n_{670} and ρ to 0.01 and 0.01 g/cm^3 or less, respectively, and typically near 0.005 and 0.005 g/cm^3. Densities, always in g/cm^3 were converted to number densities (ρ_N) with $\rho_N = \rho\ (N_A/M)$, where N_A is Avogadro's constant and M is the compound's molar mass. Number densities were needed to compute IR band strengths. Table 1 also lists other densities and refractive indices that we measured for this study. We return to these in our Section 5.

The IR spectrum of amorphous CH_3NH_2 at 10 K is shown in Fig. 1. Warming the ice at a few K/min to ~100 K

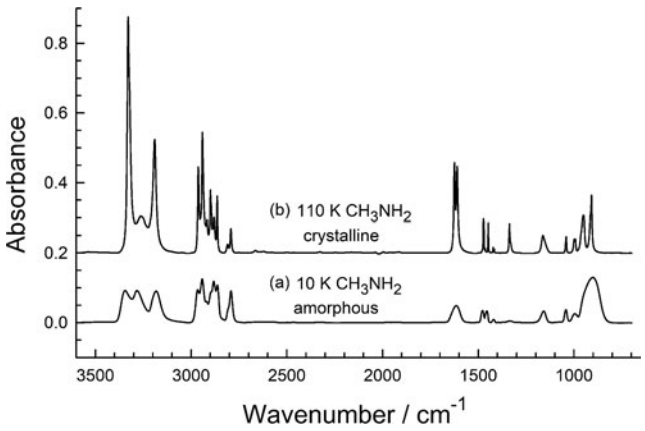

FIG. 1. IR spectra of amorphous and crystalline CH_3NH_2. Each ice was made, and its spectrum was recorded at the temperature shown in the figure. The ice sample of (a) had a thickness of about 0.97 μm, and the ice of (b) had a thickness of about 0.92 μm. Spectra are vertically offset for clarity.

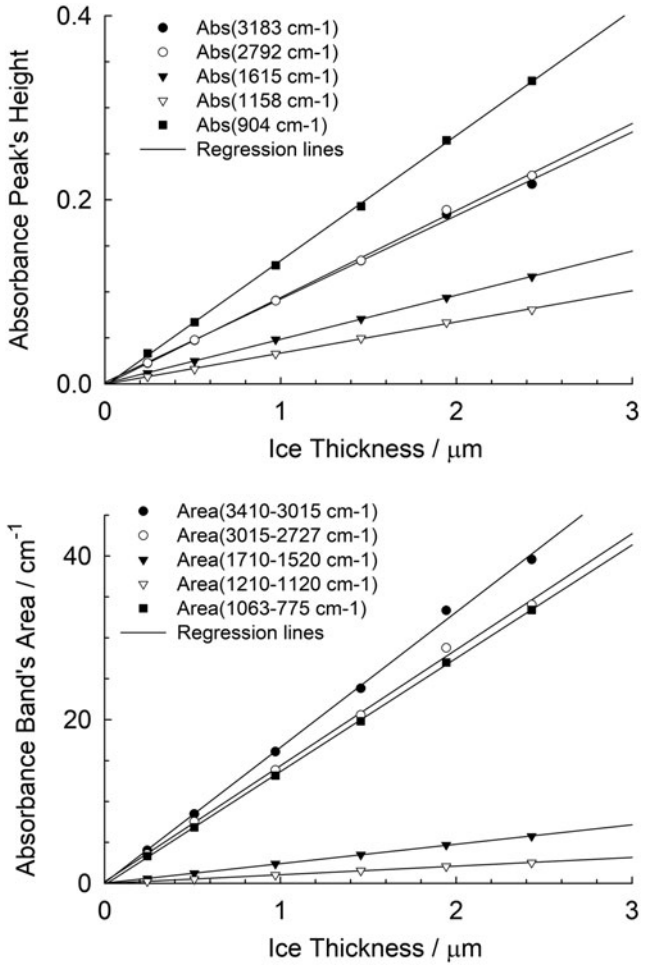

FIG. 2. Beer's Law plots for five IR features of amorphous CH_3NH_2 at 10 K.

resulted in its crystallization in about 1 min, followed by rapid sublimation on additional warming to 140 K. A faster way to make crystalline CH_3NH_2 was to vapor deposit at 110 K, which gave the crystalline ice directly. Spectra recorded by the two methods were similar, with the main difference being that peaks were sharper and better resolved below about 1650 cm^{-1} in the spectrum of the ice made at the higher temperature. A few typical Beer's Law plots are shown in Fig. 2 both for peak heights and IR band areas. Slopes of such plots were used to calculate IR absorption coefficients and band strengths with Equations (1) and (2) as already mentioned. See Table 2 for the results.

Figure 3 shows the IR spectrum of amorphous $CH_3CH_2NH_2$ at 10 K. Warming this ice sample at a few K/min to 80–90 K resulted in its crystallization, again in about 1 min, with rapid sublimation taking place at 140 K. As earlier, a faster way to make crystalline $CH_3CH_2NH_2$ was to vapor deposit at a higher temperature, in this case at 100 K. The upper trace of Fig. 3 is a typical spectrum of the crystalline solid. Once more, spectra recorded by the two methods were essentially identical and again Beer's law plots were used to derive α' and A' (Table 3).

Durig *et al.* (2006) showed that $CH_3CH_2NH_2$ exists in two conformations at ambient temperature, with about 39% of a sample of ethylamine molecules having a *trans* conformation and about 61% a *gauche* structure, and with the *trans* conformer being the more stable. See Fig. 4 for a drawing of each. Accordingly, when we prepared amorphous $CH_3CH_2NH_2$ ices by gas-phase condensation, we were freezing amine molecules with two different structures. Most vibrations of the two forms have similar IR positions (*i.e.*, wavenumber, wavelength), but a few do not. The expansion of Fig. 5 illustrates this with the IR features at 1395 and 1086 cm^{-1}, marked by asterisks in the lower trace, being for the *gauche* structure of $CH_3CH_2NH_2$. The upper trace, for the crystalline ice, shows that both peaks are absent, in

TABLE 2. POSITIONS AND INTENSITIES OF SELECTED INFRARED FEATURES OF CH_3NH_2 ICES

Form[a]	$\tilde{\nu}$ (cm^{-1})	α' (cm^{-1})	*Integration range* (cm^{-1})	A' (10^{-18} *cm molecule*$^{-1}$)
Amorphous	3183	2080	3410–3015	26.8
Amorphous	2882	2840	3015–2727	23.0
	2792	2180		
Amorphous	1615	1100	1710–1520	3.86
Amorphous	1478	765	1520–1433	1.73
	1454	735		
Amorphous	1420	191	1433–1406	0.182
Amorphous	1337	87	1378–1280	0.249
Amorphous	1159	780	1210–1120	1.71
Amorphous	904	3130	1063–775	22.5
Crystalline	3190	7070	3400–3085	42.5
Crystalline	2941	8050	3010–2832	19.0
Crystalline	2792	1900	2832–2740	1.60
Crystalline	1624	6250	1670–1525	7.63
Crystalline	1473	2180	1490–1456	0.74
Crystalline	1448	1760	1456–1433	0.297
Crystalline	1337	1930	1365–1300	1.01
Crystalline	1162	1130	1200–1110	1.74
Crystalline	1040	1110	1060–1020	0.451
Crystalline	909	3580	1020–820	9.33

[a]Amorphous ice was at 10 K, and crystalline ice was at 110 K.

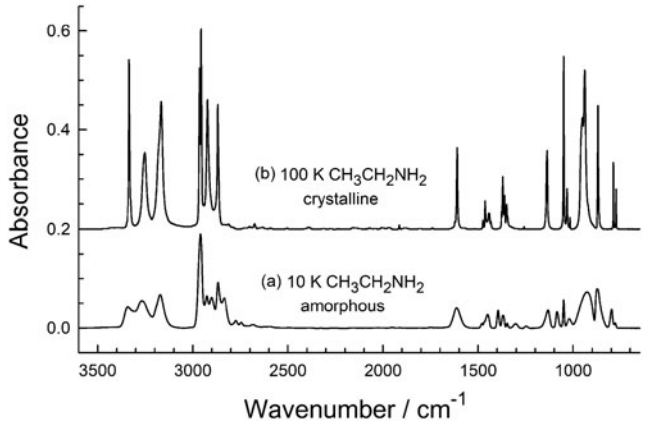

FIG. 3. IR spectra of amorphous and crystalline $CH_3CH_2NH_2$. Each ice was made, and its spectrum was recorded at the temperature shown in the figure. The ice sample of (a) had a thickness of about 0.99 μm, and the ice of (b) had a thickness of about 0.89 μm. Spectra are vertically offset for clarity.

accordance with Raman work showing that only the *trans* isomer, the more stable one, is found in crystalline ethylamine (Durig *et al.*, 2006). For another example of two conformational isomers being trapped from the gas phase, see Hudson and Coleman (2019) for our work on cyclopropanecarboxaldehyde.

In addition to absorption coefficients and band strengths, we also used optical constants $n(\tilde{\nu})$ and $k(\tilde{\nu})$ to quantify our work. Infrared optical constants are more difficult to determine than α' and A', but they allow one to calculate an IR spectrum for a range of ice thicknesses and can be used in mathematical models of planetary surfaces. We calculated optical constants by using the only free, open-source software of which we are aware, which is described in the work of Gerakines and Hudson (2020), which should be consulted for additional information. An IR spectrum can be calculated from optical constants by using the equations of Swanepoel (1983), among others, for comparison to an experimental IR spectrum.

Figures 6 and 7 are examples of the optical constants we calculated, with those shown being for amorphous methyl- and ethylamine. All of our optical constants for these amines are at https://science.gsfc.nasa.gov/691/cosmicice/constants.html. Some of the IR peaks and regions in Tables 1 and 2 involve overlapping absorbances. With our optical constants one can calculate an amine spectrum and then carry out curve fitting to deconvolve complex IR features, if needed.

5. Discussion

5.1. Comparisons to earlier work

We have not located literature values for the refractive indices and densities of our two amorphous amine ices, but X-ray diffraction studies have yielded densities of crystalline samples. Values reported are 0.850 and 0.908 g/cm^3 for crystalline methyl- and ethylamine, respectively (Atoji and Lipscomb, 1953; Maloney *et al.*, 2014), compared with our 0.880 and 0.928 g/cm^{-3}.

In a recent paper, we used molar refractions (R_M), defined by Equation (4), as a check on the consistency of our n and ρ results (Hudson *et al.*, 2020)

$$R_M = \left(\frac{M}{\rho}\right)\left(\frac{n^2-1}{n^2+2}\right), \tag{4}$$

Table 3. Positions and Intensities of Selected Infrared Features of $CH_3CH_2NH_2$ Ices

Form[a]	$\tilde{\nu}$ (cm^{-1})	α' (cm^{-1})	*Integration range* (cm^{-1})	A' (10^{-18} *cm molecule*$^{-1}$)
Amorphous	3342	995	3400–3070	24.7
	3172	1570		
Amorphous	2959	4370	3040–2525	34.1
Amorphous	1614	898	1770–1512	5.19
Amorphous	1450	584	1500–1415	1.96
Amorphous	1395	784	1415–1200	3.69
Amorphous	1132	799	1200–1103	2.49
Amorphous	1051	1190	1062–1040	1.03
Amorphous	924	1650	1040–817	18.9
	875	1750		
Amorphous	798	805	817–760	1.59
Crystalline	3335	9010	3372–3305	6.17
Crystalline	3117	6520	3305–3045	26.0
Crystalline	2956	10,200	3000–2841	25.8
Crystalline	1610	3720	1644–1590	2.44
Crystalline	1462	1330	1480–1420	1.66
Crystalline	1371	2650	1400–1300	2.91
Crystalline	1137	3980	1165–1105	2.90
Crystalline	1050	9180	1070–1010	4.55
Crystalline	939	7900	980–880	17.3
Crystalline	870	6030	878 845	2.46
Crystalline	789	3300	795–782	0.571
Crystalline	775	1850	778–770	0.306

[a]Amorphous ice was at 10 K, and crystalline ice was at 100 K.

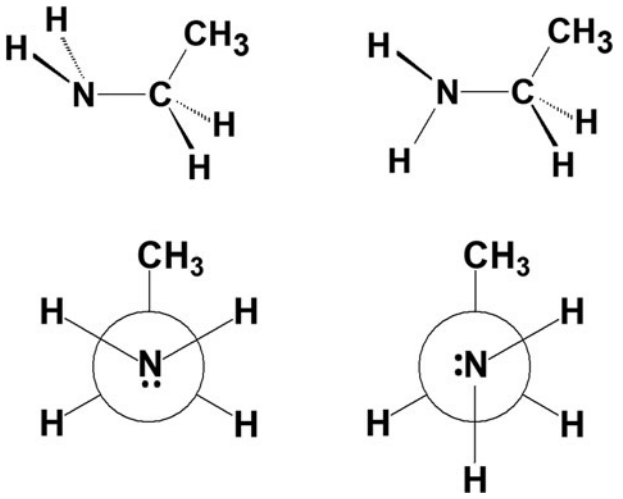

FIG. 4. The *trans* (left) and *gauche* (right) conformations of $CH_3CH_2NH_2$, ''sawhorse'' projections in the top row and Newman projections in the bottom row. As usual in the top row, solid lines represent bonds in the plane of the figure, dark solid wedges are for bonds coming out of that plane, and dashed wedges represent bonds going away from the reader.

where M, ρ, and n have the same meanings as earlier, and with measurements being made as described in Section 3. Figure 8a shows the trend in R_M on going from NH_3 to CH_3NH_2 and then to $CH_3CH_2NH_2$, each point found from data in Table 1 for an amorphous ice, the successive additions of a $-CH_2-$ group raising R_M roughly the same amount each time, as expected.

A similar graph was obtained for our crystalline compounds. Figure 8b shows that the trend in R_M for two sets of isoelectronic molecules is essentially the same, again for amorphous ices on going from a hydrocarbon to an amine to an alcohol. Not shown are similar trends for crystalline ones. These plots suggest an internal consistency in our results.

The IR spectra in our figures are in qualitative agreement with the transmission spectra we have found in the literature,

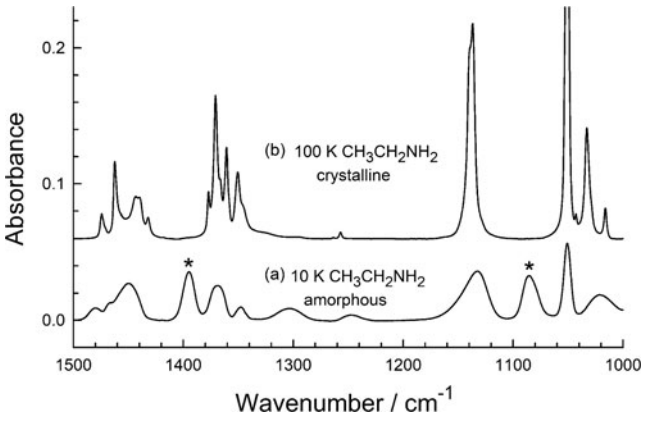

FIG. 5. Expansion of Figure 3 showing two features, each marked with an asterisk, that are present in the IR spectrum of amorphous $CH_3CH_2NH_2$, but not in the IR spectrum of the crystalline ice. Spectra are vertically offset for clarity.

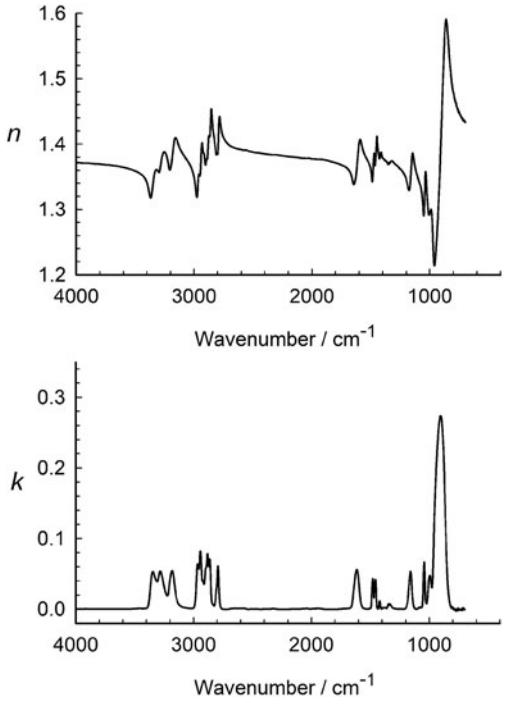

FIG. 6. Optical constants of amorphous methylamine at 10 K.

such as the transmission spectrum of crystalline CH_3NH_2 at 120 K of Durig *et al.* (1968) and the reflection spectrum of amorphous $CH_3CH_2NH_2$ of Danger *et al.* (2011). In general, peak positions, band widths, and relative intensities are similar to those seen in our own figures. Readers interested in

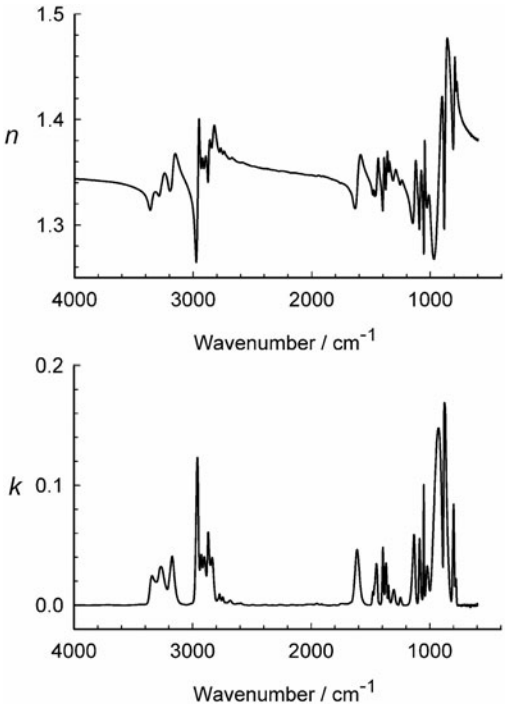

FIG. 7. Optical constants of amorphous ethylamine at 10 K.

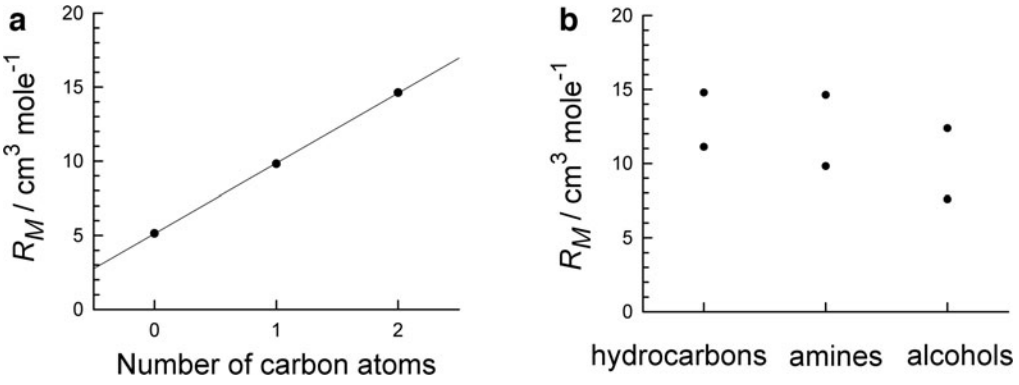

FIG. 8. **(a)** Molar refractions of, from left to right, amorphous NH_3, CH_3NH_2, and $CH_3CH_2NH_2$. **(b)** Molar refractions of two sets of isoelectronic molecules, each for an amorphous ice. The lower set of three points are from left to right, C_2H_6, CH_3NH_2, and CH_3OH, and the upper three are, again from left to right, C_3H_8, $CH_3CH_2NH_2$, and CH_3CH_2OH. See Table 1 for the n_{670}, ρ, and R_M values used for these graphs.

spectral assignments and longer lists of peak positions are urged to consult the papers just cited, keeping in mind that the IR spectra of solid amines possess a large number of overlapping features, at times making firm assignments to and interpretations of some bands controversial or uncertain (Wolff, 1970). See, for example, the uncertainty regarding the assignment and significant enhancement of the peak near 1337 cm^{-1} on going from the amorphous to the crystalline state (Durig *et al.*, 1968).

The most recent study of one of our amines is from the work of Rachid *et al.* (2021), whose transmission spectrum of amorphous CH_3NH_2 at 15 K agrees with that shown in Fig. 1 for the amorphous ice at 10 K. However, a few relative intensities, particularly below 1200 cm^{-1}, in their spectrum of the same ice after warming to 101 K to crystallize it, differ from ours in Fig. 1, with our crystalline CH_3NH_2 being made by deposition at 110 K. For example, those authors' IR peak near 905 cm^{-1} towers above all others below about 1650 cm^{-1}, which is not the case for either our spectrum or that of Durig *et al.* (1968). Such spectral differences could be due to conformational changes (rotational isomers) in crystalline CH_3NH_2 ices, as is the case with $CH_3CH_2NH_2$ (Durig *et al.*, 2006). It also could be significant that there is a substantial heat-capacity anomaly near 101 K for CH_3NH_2 (Aston *et al.*, 1937).

The only numerical comparison we have to lab data for amine ices is also from the work of Rachid *et al.* (2021) for amorphous CH_3NH_2. Their Table 2 gives six band strengths in the mid-IR region. The first two are difficult to compare with our own work, as they cover strongly overlapping features with areas that depend heavily on the choice of a baseline for integrations. However, the remaining IR bands in the work of Rachid *et al.* (2021) can be grouped into three regions and compared with results in our Table 2. Those authors' A' values are, in units of 10^{-18} cm molecule^{-1} and with our values in parentheses, roughly 1.8 (1.7), 0.2 (0.2), and 1.5 (1.7) for the 1620–1433, 1433–1406, and 1210–1120 cm^{-1} regions, respectively, which is in good agreement in all three cases. The density estimated by Rachid *et al.* (2021) using a molar refraction is only $\sim$10% lower than our measured values, which accounts for part of the difference in band strengths.

Several comparisons can be made between the IR spectra and intensities of our two amines, perhaps most easily with reference to the IR spectra of amorphous CH_3NH_2 and $CH_3CH_2NH_2$ in (a) of Figs. 1 and 3. See, for example, the similarity in the shapes and intensities (band areas) in the N–H region, corresponding to about 3400 to 3100 cm^{-1}. Conversely, an obvious difference in the two amines' spectra is in the IR intensity of the region from about 3000 to 2700 cm^{-1}, corresponding to various C–H stretching vibrations. The greater band area (*i.e.*, integrated IR intensity) found in this region in Fig. 3 simply reflects the presence of an extra CH_2 group in $CH_3CH_2NH_2$ compared with CH_3NH_2. More quantitatively, the intensity of a well-resolved peak near 1615 cm^{-1}, due to NH_2 deformation (''scissoring''), is similar for the two amorphous ices, $\sim 3.9\times10^{-18}$ and $\sim 5.2\times10^{-18}$ cm molecule^{-1} for methyl- and ethylamine, respectively. Similar intensities are also found for the large IR feature(s) for each amorphous ice near 1000 to 800 cm^{-1}, assigned to a CN stretch in each case.

Before turning to applications, we should point out that our Figs. 1 and 3 show the difficulty of identifying amines *in situ* in ices by IR methods. In particular, the extensive overlap of spectral features of CH_3NH_2 and $CH_3CH_2NH_2$ suggests that any claim of an amine detection and identification in an extraterrestrial ice should be viewed with caution. We expect gas-phase observations and meteorite analyses to be far more reliable in the study of extraterrestrial amines.

5.2. Astrobiology and applications

As just stated, IR spectra of icy mixtures can be so complex that unique assignments can be challenging. It is for this reason that we do not expect our amine results to be used by observational astronomers with either space-based or Earth-based techniques. However, the opposite expectation holds for laboratory applications. Studies of many astrobiologically relevant multi-component amine-containing ices can be proposed, but it is unrealistic and impractical to make *a priori* quantitative measurements on all of them, given the wide range of relevant variables such as composition, concentration, and temperature. However, the results

we report here can be used to help quantify any such mixture's concentration by aiding with the amine aspects of the sample preparation.

A specific example of an ice mixture of interest concerns the sort of problems mentioned in our Introduction, quantifying the low-temperature conversion of amines into amino acids by carboxylation, perhaps initiated by radiolysis or photolysis. The overall reaction for glycine formation, again as an example, is as follows:

$$CH_3NH_2 + CO_2 \rightarrow NH_2CH_2COOH \text{ (glycine)}. \quad (5)$$

The amine reactant's abundance, or its deposition (condensation) rate from the gas phase, is readily quantified by using our IR results. Improving the accuracy with which the starting material is known leads to an improvement in calculations of the glycine yield. Similar comments apply to the conversion of ethylamine to alanine.

We also note that since our tables list mid-IR intensities for multiple features of each amine then through simple scaling, one can estimate intensities of IR features beyond the mid-IR region, as in the near-IR work of Gerakines *et al.* (2005) and the far-IR work of Giulano *et al.* (2014).

In short, our work solves the problem of the unknown or uncertain band strengths of CH_3NH_2 and $CH_3CH_2NH_2$; it aids in the quantification of multi-component ices, it removes the need to use CH_3NH_2 data to quantify $CH_3CH_2NH_2$ measurements, and it can serve as baseline reference measurements for other IR regions and other temperatures.

Two other applications can be mentioned. If our amines are not held in the solid phase on, for example, the surface of a comet or an interstellar grain, then the likelihood of their conversion to amino acids drops significantly. Our band strengths can be used with the method of Khanna *et al.* (1990) to determine the vapor pressures and sublimation energies of our two amines for judging their retention on icy bodies. Our results also can serve as reference data for *ab initio* or density functional studies of IR band strengths of amorphous ices, investigations that are rarely undertaken but that could be quite useful as an alternative to time-consuming, expensive laboratory measurements.

6. IR Spectra of Amino Acids and a Recent Paper

We have already mentioned several issues and uncertainties with the paper of Iglesias-Groth and Cataldo (2021), hereafter denoted IGC21. Here, we comment on three other concerns. First, the astrobiological or extraterrestrial environment to which the results of IGC21 apply is not clearly stated. The IR spectra presented are for amino acids isolated in solid matrices, so presumably the relevance is to extraterrestrial solids, and specifically to ices. Mention is made several times of possible astronomical observations of the amino-acid IR features presented, but since the IR spectra of interstellar and planetary ices are dominated by just a few molecules (*e.g.*, H_2O, CO_2, CO, CH_3OH); then, IR features of amino acids, with their low abundance, would be essentially invisible. Further, the IR spectra of amino acids, such as those of our amines, suffer such extensive overlap with one another that a solid-phase identification is impossible with present technology.

A second concern with IGC21 is that the IR samples were prepared by starting with room-temperature crystalline amino acids, and so in each case the amino acid was in the zwitterionic form. However, it is not certain that amino acids in interstellar ices will be zwitterionic. A non-zwitterionic structure is expected for the gas phase, which we and others have shown can be trapped in solids (Gomez-Zavaglia and Fausto, 2003; Gerakines and Hudson, 2013). For the case of Europa, with acidic conditions, protonated amino acids are more likely, but deprotonated amino acids could be more important in nitrogen-rich environments such as Titan, where NH_3 and amines could be present.

Finally, the authors of IGC21 suggest that the agreement of some of their IR intensities with earlier work in aqueous solution (Wolpert and Hellwig, 2006) supports the accuracy of their own results, but there is no particular reason to expect quantitative agreement between measurements made with anhydrous solid-phase amino acids and those same compounds in aqueous solution. Further, the authors selected only two to four IR features for each amino acid on which to base their comment about agreement and accuracy. A stronger comparison would include more of the dozen or so IR peaks for each compound. We also point out that in the earlier work (Wolpert and Hellwig, 2006), pH values as low 0.3 and as high as 11.0 were used for four of the five amino acids later studied in zwitterionic crystalline form in IGC21. Only in the case of glycine could one safely assume a similarity in molecular structure in the aqueous sample studied, which had pH 6.2, and glycine embedded in CsI or polyethylene.

Having said all of this, we end on a more positive note for future work. To our knowledge, reliable IR intensities for amino acids have yet to be measured in the solid phase. Preparation of amino-acid samples in alkali halide pellets could be useful, but only if the samples' spectra were shown to obey Beer's Law and not be resolution limited. Another suggestion is to prepare solid-phase samples by vapor-phase deposition of amino acids in more relevant matrices, such as H_2O-ice or CO_2-ice, measure their IR transmission spectra, and then follow the procedures we have described here for amines, a task that could be both tedious and time-consuming, but the results could be a valuable addition to the literature.

Acknowledgments

Y.Y.Y. thanks the NASA Postdoctoral Program for her fellowship.

Author Disclosure Statement

No competing financial interests exist.

Funding Information

Funding from NASA's Planetary Science Division Internal Scientist Funding Program through the Fundamental Laboratory Research (FLaRe) work package at the NASA Goddard Space Flight Center is acknowledged.

References

Altwegg K, Balsiger H, Bar-Nun A, *et al.* (2016) Prebiotic chemicals—amino acid and phosphorus—in the coma of comet 67P/Churyumov-Gerasimenko. *Sci Adv* 2:1.

Aponte JC, Abreu NM, Glavin DP, *et al*. (2017) Distribution of aliphatic amines in CO, CV, and CK carbonaceous chondrites and relation to mineralogy and processing history. *Meteorit Planet Sci* 52:2632–2646.

Aston JG, Siller CW, and Messerly GH (1937) Heat capacities and entropies of organic compounds. III. Methylamine from 11.5°K to the boiling point. Heat of vaporization and vapor pressure. The entropy from molecular data. *J Am Chem Soc* 59:1743–1751.

Atoji M and Lipscomb WN (1953) On the crystal structures of methylamine. *Acta Cryst* 6:770–774.

Danger G, Bossa JB, de Marcellus P, *et al*. (2011) Experimental investigation of nitrile formation from VUV photochemistry of interstellar ices analogs: acetonitrile and amino acetonitrile. *Astron Astrophys* 525:A30.

de la Paz LR and Getoff N (1966) Cobalt-60 gamma-ray-induced carboxylation of methylamine. *Radiat Res* 28:567–575.

Durig JR, Bush SF, and Baglin FG (1968) Infrared and Raman investigation of condensed phases of methylamine and its deuterium derivatives. *J Chem Phys* 49:2106–2117.

Durig JR, Zheng C, Gounev TK, *et al*. (2006) Conformational stability from temperature-dependent Fourier transform infrared spectra of noble gas solutions, r_0 structural parameters, and barriers to internal rotation for ethylamine. *J Phys Chem A* 110:5674–5684.

Gerakines PA and Hudson RL (2013) Glycine's radiolytic destruction in ices: first in situ laboratory measurements for Mars. *Astrobiology* 13:647–655.

Gerakines PA and Hudson RL (2015) The radiation stability of glycine in solid CO_{2-} in situ laboratory measurements with applications to Mars. *Icarus* 252:466–472.

Gerakines PA and Hudson RL (2020) A modified algorithm and open-source computational package for the determination of infrared optical constants relevant to astrophysics. *Astrophys J* 901:1.

Gerakines PA, Hudson RL, Moore MH, *et al*. (2012) In-situ measurements of the radiation stability of amino acids at 15–140 K. *Icarus* 220:647–659.

Getoff N and Schenck GO (1967) On the formation of amino acids by gamma-ray-indiced carboxylation of amines in aqueous solutions. *Radiat Res* 31:486–505.

Giulano BM, Escribano RM, Martin-Doménech R, *et al*. (2014) Interstellar ice analogs: band strengths of H_2O, CO_2, CH_3OH, and NH_3 in the far-infrared region. *Astron Astrophys* 565: A108.

Glavin DP, Dworkin JP, and Sandford SA (2008) Detection of cometary amines in samples returned by Stardust. *Meteorit Planet Sci* 43:399–413.

Gomez-Zavaglia A and Fausto R (2003) Low-temperature solid-state FTIR study of glycine, sarcosine and *N*,*N*-dimethylglycine: observation of neutral forms of simple α-amino acids in the solid state. *Phys Chem Chem Phys* 5: 3154–3161.

Heavens OS (1955/2011) *Optical Properties of Thin Solid Films*, 2nd ed., Butterworths Scientific Publications and Dover, London and New York, p. 114.

Holtom PD, Bennett CJ, Osamura Y, *et al*. (2005) A combined experimental and theoretical study on the formation of the amino acid glycine (NH_2CH_2COOH) and its isomer ($CH_3NHCOOH$) in extraterrestrial ices. *Astrophys J* 626:940–952.

Hudson RL and Coleman FM (2019) Solid-state isomerization and infrared band strengths of two conformational isomers of cyclopropanecarboxaldehyde, a candidate interstellar molecule. *ACS Earth Space Chem* 3:1182–1188.

Hudson RL, Lewis AS, Moore MH, *et al*. (2009) Enigmatic isovaline: investigating the stability, racemization, and formation of a non-biological meteoritic amino acid. In *Bioastronomy 2007: Molecules, Microbes, and Extraterrestrial Life*, edited by K.J. Meech, J.V. Keane, M.J. Mumma, J.L. Siefert, and D.J. Wertheimer. Astronomical Society of the Pacific, San Francisco, California.

Hudson RL, Ferrante RF, and Moore MH (2014a) Infrared spectra and optical constants of astronomical ices: i. amorphous and crystalline acetylene. *Icarus* 228:276–287.

Hudson RL, Gerakines PA, and Moore MH (2014b) Infrared spectra and optical constants of astronomical ices: II. ethane and ethylene. *Icarus* 243:148–157.

Hudson RL, Loeffler MJ, and Gerakines PA (2017) Infrared spectra and band strengths of amorphous and crystalline N_2O. *J Chem Phys* 146:0243304.

Hudson RL, Loeffler MJ, Ferrante RF, *et al*. (2020) Testing densities and refractive indices of extraterrestrial ice components using molecular structures—organic compounds and molar refractions. *Astrophys J* 891:1–10.

Hudson RL, Yarnall YY, Gerakines PA, *et al*. (2021) Infrared spectra and optical constants of astronomical ices: III. Propane, propylene, and propyne. *Icarus* 354:14033.

Iglesias-Groth S and Cataldo F (2021) Integrated molar absorptivity of mid- and far-infrared spectra of glycine and other selected amino acids. *Astrobiology* 21:526–540.

Kaifu N, Morimoto M, Nagane K, *et al*. (1974) Detection of interstellar methylamine. *Astrophys J* 191:L135–L137.

Khanna RL, Allen Jr, JE, Masterson CM, *et al*. (1990) Thin-film infrared spectroscopic method for low-temperature vapor pressure measurements. *J Phys Chem* 94:440–442.

Mahjoub A and Hodyss R (2018) Thermal reaction in cometary and pre-cometary ices: formation of thiocarbamate in OCS-CH_3NH_2 mixed ices. *Astrophys J* 869:1–6.

Maloney AGP, Wood PA, and Parsons S (2014) Competition between hydrogen bonding and dispersion interactions in the crystal structures of the primary amines. *CrystEngComm* 16: 3867–3882.

Materese CK, Gerakines PA, and Hudson RL (2021) Laboratory studies of astronomical ices—reaction chemistry and spectroscopy. *Acc Chem Res* 54:280–290.

Mayerhoöfer TG, Pahlow S, and Popp J (2020) The Bouguer-Beer-Lambert law: shining light on the obscure. *ChemPhysChem* 21:2029–2046.

Moore MH, Ferrante RF, Moore WJ, *et al.* (2010) Infrared spectra and optical constants of nitrile ices relevant to Titan's atmosphere. *Astrophys J Suppl Ser* 191:96–112.

Rachid MG, Brunken N, de Boe D, *et al*. (2021) Infrared spectra of complex organic molecules in astronomically relevant ice mixtures. *Astron Astrophys* 653:1–33.

Swanepoel R (1983) Determination of the thickness and optical constants of amorphous silicon. *J Phys E Sci Instrum* 16: 1214–1222.

Swenson CA, Person WB, Dows DA, *et al*. (1959) Infrared studies of crystal benzene. I. the resolution and assignment of v_{20}, and the relative magnitudes of crystal fields in benzene. *J Chem Phys* 31:1324–1328.

Vinogradoff V, Duvernay F, Danger G, *et al*. (2013) Formaldehyde and methylamine reactivity in interstellar ice analogues as a source of molecular complexity at low temperature. *Astron Astrophys* 549:A40.

Wolff H (1970) Infrared and Raman investigation of condensed phases of methylamine and its deuterium derivatives. *J Chem Phys* 52:2800–2802.

Wolpert M and Hellwig P (2006) Infrared spectra and molar absorption coefficients of the 20 alpha amino acids in aqueous solutions in the spectral range from 1800 to 500 cm^{-1}. *Spectrochim Acta A* 64:987–1001.

Address correspondence to:
Reggie L. Hudson
Astrochemistry Laboratory (Code 691)
NASA Goddard Space Flight Center
Greenbelt, MD 20771
USA

E-mail: reggie.hudson@nasa.gov

Submitted 19 August 2021
Accepted 6 December 2021
Associate Editor: Christopher McKay

Abbreviation Used

IR = infrared